J Mater Sci: Mater Med (2010) 21:2793–2804
DOI 10.1007/s10856-010-4129-y

Poly(2-hydroxyethyl methacrylate-co-dodecyl methacrylate-co-acrylic acid): synthesis, physico-chemical characterisation and nafcillin carrier

Teodora Zecheru · Traian Rotariu · Edina Rusen · Bogdan Mărculescu · Florin Miculescu · Laura Alexandrescu · Iulian Antoniac · Izabela-Cristina Stancu

Received: 25 January 2010 / Accepted: 5 July 2010 / Published online: 22 July 2010

Abstract In the present study polymeric microbeads of poly(2-hydroxyethyl methacrylate-co-dodecyl methacrylate-co-acrylic acid) or p(HEMA-co-dDMA-co-AA) were synthesised and characterized through FT-IR and scanning electron microscopy (SEM); their swelling behavior against saline solution was explored and their in vitro cytotoxicity was evaluated. Further, in order to elucidate kinetic aspects regarding the ternary system p(HEMA-co-dDMA-co-AA), a mathematical model of the reactivity ratios of the comonomers in the terpolymer has been conceived and analyzed. An intensified tendency of AA units accumulation in the copolymer has been noticed, in spite of HEMA units, while dDMA conserves in the copolymer the fraction from the feed. Three compositions have been selected for nafcillin-loading and their in vitro release capacity was evaluated. The compositions of 80:10:10 and 75:10:15 M ratios appear suitable for further in vivo testing, in order to be used as drug delivery systems in the treatment of different osseous diseases.

T. Zecheru · E. Rusen · B. Mărculescu · F. Miculescu · L. Alexandrescu · I. Antoniac · I.-C. Stancu (✉)
University Politehnica of Bucharest, 149 Calea Victoriei, 010072 Bucharest, Romania
e-mail: izabela.cristina.stancu@gmail.com

T. Zecheru
CBRN Defense and Ecology Scientific Research Center, 225 Şos. Olteniţei, 041309 Bucharest, Romania

T. Rotariu
Military Technical Academy, 81-83 Bd. George Coşbuc, 050141 Bucharest, Romania

1 Introduction

In the last few years, polymeric materials have been designed and proposed as matrices or depot systems for injectable or implantable systems or devices [1–7]. A particular approach towards an improved use of drugs for therapeutic applications is the design of polymeric prodrugs or polymer–drug conjugates. Polymer chemists started to link drugs to polymers in order to improve their efficiency since the 1950s. At that time, they were mainly focusing on the chemistry itself, and different classes of polymers were covalently combined with a variety of drugs. The biological aspects for the design of polymeric prodrugs were hardly taken into consideration.

The first rational model for pharmacologically active polymers was proposed by Ringsdorf in 1975 [8], who recognized the immense potential of polymeric prodrugs. The model mainly consisted of five components: the polymeric backbone, the drug, the spacer, the targeting group, and the solubilizing agent. The polymeric carrier can be either an inert polymer or a biodegradable polymer. The drug can be fixed directly or via a spacer group onto the polymer backbone. The proper selection of this spacer brings the opportunity of controlling the site and the rate of release of the active drug from the conjugate by hydrolytic or enzymatic cleavage.

Treatment of osteomyelitis in most patients requires a lengthy regimen of parenteral antibiotic therapy and surgical removal of all necrotic, avascular, infected bone and soft tissue. Optimally, culture-directed antimicrobial therapy should be initiated after complete surgical debridement and after microbial confirmation of the diagnosis by biopsy [9, 10]. Generally, antibiotic therapy is maintained for at least 5 days. Inadequate debridement is a frequent

underlying factor in therapy failure in patients with chronic osteomyelitis.

4-Thia-1-azabicyclo[3.2.0]heptane-2-carboxylic acid, 6-[[(2-ethoxy-1-naphtalenyl)-carbonyl]-amino]-3,3-dimethyl-7-oxo-, monosodium salt, monohydrate, [2S-(2^{α}, 5^{α}, 6^{β})] or nafcillin, is a semi-synthetic antistaphylococcal penicillin, highly effective in penicillinase-producing staphylococcal infections, in which activity is conferred mainly by steric hindrance. Unlike penicillin, ampicillin, or the extended-spectrum penicillins, nafcillin resists hydrolysis by penicillinase. As a result, nafcillin, along with other agents in the same group (e.g., oxacillin, dicloxacillin), is active against penicillinase-producing *Staphylococcus aureus* [9–12]. Nafcillin, because of its side chain, resists destruction by beta-lactamases. This makes it useful for treating bacteria that resist penicillin due to the presence of penicillinase. Nowadays, nafcillin is employed in invasive diseases due to *Enterobacter cloacae* and *Serratia marcescens* [10, 13].

Polymer–drug conjugates and especially polymer-nafcillin compounds were synthesized as hydrogels or beads, and their in vitro behavior properties were studied, such as pMMA, p(MMA-co-AA) [12–14], poly(*N*-isopropyl-acrylamide-co-itaconic acid) [15], but the influence of some factors, such as: the synthesis method, the crosslinking agent, the solvent and others, in the structure of the hydrogel, make difficult to compare the diffusion coefficients either from hydrogels or particles.

Nafcillin works by penicillin-binding proteins and inhibiting the cross-linking of cell wall peptidoglycan. This antibiotic is especially useful to treat infections caused by methycillin-sensitive penicillinase-producing staphylococci. The offending bacteria can be successfully treated anywhere including bone, joint, urinary tract, respiratory tract, skin, endocarditis, meningitis. However, with serious infections such as those just described, intravenous administration is recommended [16–21].

In this context, the present study was (1) devoted to the development of a new polymer-based nafcillin carrier system consisting in terpolymer microbeads of poly(2-hydroxyethyl methacrylate-co-dodecyl methacrylate-co-acrylic acid) or p(HEMA-co-dDMA-co-AA) and (2) to the corresponding drug immobilization and in vitro release assessment. In this respect, polymeric microbeads have been synthesized and characterized (using FT-IR, scanning electron microscopy (SEM), swelling behavior and in vitro cytotoxicity tests). In the aim of better understanding and control the structure and properties of the copolymer microparticles, the study has been completed with the kinetic analysis of two binary systems (HEMA-AA and AA-dDMA), the third one (HEMA-dDMA) being already described in the literature [14]. The composition of the synthesized terpolymer is extremely important due to the fact that the carboxyl groups from AA structural units bring important kinetic modifications for Nafcillin linkage and release. It is easy to anticipate that the total content and the distribution pattern of these functionalities in the macromolecular backbone represent important characteristics of the polymeric support in the context of this particular approach. This is the fundamental reason for the investigations of the kinetic parameters governing the synthesis process and the properties of the obtained copolymers.

The second part of the work has been aimed at the antibiotic loading in the so-formed particles; three compositions were loaded in order to evaluate their in vitro drug-release capacity.

2 Experimental

2.1 Materials

The monomers 2-hydroxyethyl methacrylate (HEMA), dodecyl methacrylate (dDMA) and acrylic acid (AA), were purchased from Sigma-Aldrich. HEMA was distilled under reduced pressure (67°C and 3.5 mbar), and the other monomers were passed through a column packed to a height of 20 cm with basic Al_2O_3 (Merck). The initiator, benzoyl peroxide (BPO) (Merck) was purified by recrystallization from ethanol. 2-butanol (BUT) (Aldrich), toluene (T) and diethyl ether (DEET) were provided from Chimopar, and the star copolymer styrene-butadiene (pBuSt), as stabilising agent, from ICECHIM Bucharest. Ethylene glycol dimethacrylate (EGDMA) (Merck), the cross-linking agent, was used as received. The solvents used were dioxane (D) (Fluka) and *N*,*N*-dimethylformamide (DMF) (Aldrich). D has been distilled on metallic Na and stored on molecular sieves (4 Å) (Merck); DMF (Aldrich) was kept on molecular sieves (4 Å) after distillation under reduced pressure ($p = 30$ mmHg, $T = 60$°C). Nafcillin (NFPC) and *N*,*N*′-dicyclohexyl carbodiimide (DCC) (both from Merck) were used without further purification.

The substances for the in vitro tests were: Dulbecco's Modified Eagle Medium (DMEM)-culture medium (Eurobio, France), 3–4, 5 dimethylthiazole-2-yl)-2, 5-diphenyl-tetrazolium bromide (MTT)-labeling agent, penicillin and streptomycin-antibiotics (Sigma).

2.2 Polymer synthesis

2.2.1 Polymerisation procedures for obtaining microbeads

A solution of stabilising agent in T (5:95 (w/v) vs. monomer) has been introduced into a three-neck reactor, BUT (45:55 (v/v) ratio of solvent vs. non-solvent solution) was slowly introduced at 40°C and while stirring. Separately, a solution containing the monomers (Table 1), BPO

Table 1 Molar composition of the initial mixture of monomers

Sample	HEMA	dDMA	AA
A1	90	5	5
A2	85	5	10
A3	80	5	15
A4	85	10	5
A5	80	10	10
A6	75	10	15

(5×10^{-3} mol/l in the solution), and the cross-linking agent (EGDMA) (2% molar vs. monomers) has been prepared. This second solution has been dropwise added to the first one, under mechanical stirring, while increasing the temperature to 75°C and the stirring rate to 800 rpm. Polymerisations have been performed in a water-bath and under nitrogen atmosphere. An optimal result of the reaction and a high conversion was noticed after 6–7 h. The terpolymers obtained were repeatedly washed with T and DEET and extracted under centrifugation, in order to remove any traces of unreacted monomer and other organic residue with low molecular weight. Then the microbeads have been dried in the oven at 37°C for 24 h under reduce pressure (30 mmHg).

2.2.2 Polymerisation procedures for kinetic tests

Polymerisation tests have been carried out in vials and under nitrogen. The following pairs of monomers have been studied: HEMA (as M_1)-AA (as M_2) and AA (as M_1)-dDMA (as M_2). Monomers solutions of 1.5 mol/l concentration have been prepared with the molar ratio among the comonomers given in Table 2. The monomers, the solvent and the initiator (5×10^{-3} mol/l) constitute the polymer solution. Four polymerisation test tubes are used for each composition, in order to determine different conversions, and the tests were performed in triplicate. The polymer obtained was precipitated using an adequate non-solvent. The solid products obtained have been washed several times with the same non-solvent, in order to remove residual monomers, and dried in a vacuum oven up to constant mass and weighted.

Table 2 Feed compositions of the binary systems used for the kinetic copolymerization study

Composition	Monomer 1	Monomer 2
1	0.2	0.8
2	0.4	0.6
3	0.6	0.4
4	0.8	0.2

2.3 Characterization

2.3.1 Polymer characterization

The terpolymers have been subjected to infrared (FT-IR) spectroscopy. The analyses were performed on solid dried samples, with a Jasco FT-IR 6200 equipped with a SPECAC Golden Gate ATR accessory. The polyhydroxyethyl methacrylate homopolymer (pHEMA) has been used as control. Morphology studies of both NFPC-loaded and non-loaded terpolymer microbeads have been performed through SEM using a Philips XL30-ESEM turbo molecular pump (TMP), at 20 keV. The synthesized copolymers were subjected to elemental analysis using a C–H–N analyzer EAGER 200, Stripchart.

2.3.2 Kinetic copolymerization study

Taking into consideration that a terpolymerisation is in discussion, Eqs. 1 and 2 of Alfrey–Merz–Goldfinger are applied for the composition determination [22].

$$\frac{d[M_1]}{d[M_2]} = \frac{[M_1]\left([M_1] + \frac{[M_2]}{r_{12}} + \frac{[M_3]}{r_{13}}\right)\left(\frac{[M_1]}{r_{21}r_{31}} + \frac{[M_2]}{r_{21}r_{32}} + \frac{[M_3]}{r_{31}r_{23}}\right)}{[M_2]\left(\frac{[M_1]}{r_{21}} + [M_2] + \frac{[M_3]}{r_{23}}\right)\left(\frac{[M_1]}{r_{12}r_{31}} + \frac{[M_2]}{r_{12}r_{32}} + \frac{[M_3]}{r_{32}r_{13}}\right)} \quad (1)$$

$$\frac{d[M_2]}{d[M_3]} = \frac{[M_2]\left(\frac{[M_1]}{r_{21}} + [M_2] + \frac{[M_3]}{r_{23}}\right)\left(\frac{[M_1]}{r_{12}r_{31}} + \frac{[M_2]}{r_{12}r_{32}} + \frac{[M_3]}{r_{32}r_{13}}\right)}{[M_3]\left(\frac{[M_1]}{r_{31}} + \frac{[M_2]}{r_{32}} + [M_3]\right)\left(\frac{[M_1]}{r_{13}r_{21}} + \frac{[M_2]}{r_{23}r_{12}} + \frac{[M_3]}{r_{13}r_{23}}\right)} \quad (2)$$

where
$r_{12} = \frac{k_{11}}{k_{12}}$; $r_{21} = \frac{k_{22}}{k_{21}}$; $r_{23} = \frac{k_{22}}{k_{23}}$; $r_{32} = \frac{k_{33}}{k_{32}}$; $r_{13} = \frac{k_{11}}{k_{13}}$; $r_{31} = \frac{k_{33}}{k_{31}}$.

The reactivity ratios pairs r_{ij} and r_{ji} are basically r_i and r_j from the binary copolymerization M_i/M_j[10–13]. Therefore, in order to be able to solve the above Eqs. 1 and 2, the determination of the six reactivity ratios obtained from the composition analyses (elemental analysis) of the three derived binary systems is mandatory.

2.3.3 Assessment of the swelling behaviour

The swelling behavior of the obtained terpolymers represents an important parameter for the study of the structures compatibility with physiological fluids. Swelling tests were carried out on terpolymer samples obtained as cross-linked hydrophilic matrices by bulk polymerisation, using the same composition as previously mentioned (see Table 1), after the immersion in a saline solution mimicking the human serum (9 g/l NaCl in distilled water), for 3 days at 37°C. The homopolymer (pHEMA) (obtained using the same procedure as for the terpolymers) was used as control.

All the measurements were performed in triplicate for each polymer series, through the immersion of the polymer discs in 50 ml solution. The swelling degrees were assessed using the blot-and-weight technique. The dry weights of the samples (W_d) were determined prior the immersion in saline solution. After samples' removal from the solution, at different time intervals, disks were gently blotted to remove the saline excess and then weighted to obtain the wet weight (W_w); after the measurement, the samples were reintroduced in saline to continue their swelling process. The swelling degree was evaluated using the equation:

$$Swelling\ degree = \frac{W_w - W_d}{W_d} \cdot 100. \quad (3)$$

2.4 Coupling reaction of NFPC

The coupling procedure of the antibiotic on the terpolymers has been adapted from a method described in the literature [23]. Briefly, 1.54 g (3.4 mmol) of NFPC were dissolved in 7 ml of DMF, in a two-necked flask containing two dropping funnels, and the flask was cooled to 0–5°C with an ice-water bath. Then, 0.72 g (3.5 mmol) of DCC were dissolved in 7 ml of DMF and added dropwise to the solution of the flask through the first dropping funnel. The solution obtained was stirred at 0–5°C for 10 min. In another dropping funnel, 1.0 g (6.8 mmol) of p(HEMA-co-dDMA-co-AA) (accordingly to the total conversion of the comonomers) was introduced in 10 ml of DMF and added dropwise under stirring to the solution in the flask. The mixture was stirred overnight, and the white precipitate produced was filtered, collected, washed with cooled ethanol, and dried in vacuo at room temperature for 24 h. The success of the drug loading has been first qualitatively explored through FT-IR spectroscopy (using a Jasco FT-IR 6200 equipped with a SPECAC Golden Gate ATR accessory). The drug-loaded polymers have been assessed against NFPC and the corresponding non-loaded terpolymers, in order to prove the success of antibiotic immobilization. Moreover, the quantitative measurement of NFPC in the drug-loaded terpolymers was performed through UV–Vis spectroscopy (using a GBC Cintra 303 apparatus at a fixed wavelength of 330 nm). Briefly, to destroy the chemical linkage between NFPC and the carrier, 0.02 g of drug-terpolymer compounds have been suspended in 8 ml methanol. Subsequently the samples have been vigorously vortexed and the terpolymers have been separated by centrifugation (4000 rpm for 10 min). Then the supernatant has been used for absorbance measurement at 330 nm. Drug content has been determined against a standard curve obtained using NFPC solutions in methanol with known concentrations (between 0.001 and 0.1 mg/ml).

Additionally, SEM assessment has been performed to morphologically verify whether the microbeads were agglomerated or damaged in shape following the drug-loading procedure.

2.5 Hydrolysis and drug release procedures

Polymer–drug compounds (100 mg) were poured into 10 ml of saline aqueous solution (9 g/l NaCl in distilled water) at 37°C, and the mixtures were placed in cellophane membrane dialysis tubes (Sigma). The tubes were closed and introduced into flasks containing 200 ml of the saline solution maintained at 37°C. Three milliliter samples were removed at selected intervals, and 3 ml of the saline solution were replaced. The drug released was detected through UV–Vis spectroscopy (using a GBC Cintra 303 apparatus at a fixed wavelength of 330 nm and 37°C) and the quantity was determined from the calibration curve obtained for saline solutions of NFPC with known concentrations. Each experiment was performed in triplicate.

2.6 Biologic evaluation

Polymers biocompatibility was assessed through in vitro cytotoxicity and cells viability tests. The polymer pellets have been sterilized through exposure to UV light, at 360 nm and 12 W for 8 h. The protocol was previously described thoroughly [24].

In order to obtain a homogenous distribution, murine fibroblast L929 cell line was cultivated at a confluence of 25% of the surface in 24 well-plates of 1000 µl/well and incubated for 72 h at 37°C, in humidified atmosphere containing 5% CO_2. At a 95% microscopically observed confluence, the culture medium DMEM was replaced with 1000 µl DMEM supplemented with 10% calf foetal serum, 1% L-glutamine and antibiotics (penicillin and streptomycin) at 37°C. The cells culture containing the polymer samples was afterwards incubated in standard polystyrene 24-well plates (1 polymer pellet of $\sim$1 g/well) in thermostat at 37°C, in the presence of 5% CO_2 and was microscopically examined daily during 3 days for detecting cytotoxicity visible signs, cellular lysis or cellular components dimensions and conformation. Meanwhile, a control experiment was performed.

For the cytotoxicity evaluation, cellular viability was determined with MTT, which was added to the polymers in the last 4 h of the culture period (100 µl/well from a 5 mg/ml solution in TFS), until violet crystals of formazan appeared. Optical density was read at 570 nm using an automatic microplate reader (ELISA). The relative cell viability was determined as percentage of the optical densities in the medium containing serially diluted concentrations to the optical densities in the control medium. The cell number containing violet crystals of formazan was estimated through the analysis of images taken from an

inverse microscope ZEISS Axiovert through ImageJ software analysis. The number of living cells is directly proportional with the level of formazan obtained.

3 Results and discussion

3.1 FT-IR analysis of the terpolymers

The first stage in the approach of this study has been represented by the FT-IR analysis of the terpolymers obtained. Since all the copolymers have been prepared with high ratios of HEMA units, a strong and broad vibration in the region of 3500–3300 cm^{-1} was expected to occur, corresponding to the O–H stretching. The AA units should also contribute with a broad band that generally extends from 3300 to 2500 cm^{-1}. This was consistent with the experimental results: all the terpolymers presented strong and very broad vibrations at about 3426–3393 cm^{-1}; the signal has been assigned to the coupled O–H signals of mixed origin, from the HEMA units and from the AA units. Moreover, when compared to the control spectrum of p(HEMA), a shifting to the right has been noticed, proving the presence of the O–H vibration of carboxylic origin from AA. Similarly, the three structural units of the terpolymers are responsible for the strong vibration recorded at 1716 cm^{-1}. This is assigned to the mixed contribution of the C=O stretching vibration from AA, HEMA and dDMA; the coupled influence of the three type of C=O vibration has generated a little shifting when compared to the spectrum of p(HEMA), where the carbonyl appears at 1729 cm^{-1}. Nevertheless, with respect to p(HEMA), the presence of carbonyl groups in all the three types of structural units has lead to a strong increase of the intensity of the C=O band at 1716 cm^{-1} when compared to the O–H stretching vibration band at about 3400 cm^{-1}. This is evident since in p(HEMA) the molar ration between O–H and C=O is 1:1, while in the analysed terpolymers, the C=O groups exceed the OH functionalities (due to the presence of dDMA that contains carbonyl group, but no hydroxyl). Figure 1 selectively presents the spectra of two terpolymers, A3 and A4 against the control spectrum of p(HEMA). It can be concluded that the FT-IR assessment has successfully confirmed the presence of the three structural units in the final terpolymers.

3.2 SEM analysis

Since particles' dimension represents a very important parameter depending on the type of biomedical application, the next stage of this study has consisted in SEM morphological investigation of the obtained terpolymers. The images from Fig. 2 show that all the polymers synthesized have been obtained as round shaped particles with dimensions of ~ 1 μm. The use of different ratios of the three comonomers in the polymerization mixtures had no effect on the shape, dimension or other visible characteristics of the terpolymer beads. A narrow dimensional dispersion of the particles has been generally noticed. Therefore, all the microbeads are morphologically appropriate to be further used as drug delivery matrices.

3.3 Kinetic copolymerization study

3.3.1 Kinetic study of p(HEMA-co-AA) binary system

The analysis of the binary system HEMA-AA has begun from the elemental analysis results presented in Table 3. The reactivity ratios estimated using PROCOP [25, 26] software have been determined to be: $r_1 = 0.00029$ and $r_2 = 0.148$ (M_1 = HEMA, M_2 = AA). These values have enabled plotting the instantaneous composition diagram for the system, which is characterized by $r_1 < 1$ and $r_2 < 1$ (Fig. 3a). Conversion-time dependence for HEMA-AA binary system copolymerization is presented below (Fig. 3b). The analysis of the graph in Fig. 3 has led to the conclusion that the ratio among the two monomers in the feed did not substantially influence the copolymerization rate.

3.3.2 Kinetic study of p(AA-co-dDMA) binary system

The system AA-dDMA has been analyzed starting from the experimental data obtained through the elemental analysis (data not shown). Being known the feed composition, the compositions and conversions of the copolymers obtained, PROCOP software has been further used to determine the reactivity ratios. The penultimate effect has been considered for the kinetic model (eight types of propagation reactions) due to sterical effects (the volume of dDMA), which affects the macroradicals reactivity.

Notations: M_1 = AA, M_2 = dDMA.

The values obtained using the software are: $r_{11} = 0.02099$; $r_{22} = 0.12933$; $r_{21} = 0.13121$; $r_{12} = 4.83283$. Using Berger and Kunz equation [27], average values of r_1 and r_2 have been calculated. The values obtained are: $\overline{r_1} = 0.108$; $\overline{r_2} = 0.63$. The plotting of composition diagram for the AA-dDMA binary system has been performed knowing the values of the reactivity ratios (Fig. 4a). The analysis of the above-mentioned diagram has suggested a typical behavior of a $r_1 < 1$ and $r_2 < 1$ system. The dependence conversion versus time for the copolymerization of AA-dDMA binary system is presented in Fig. 4b. In this case, the ratio among the two monomers in the feed has a substantial influence on the copolymerization rate.

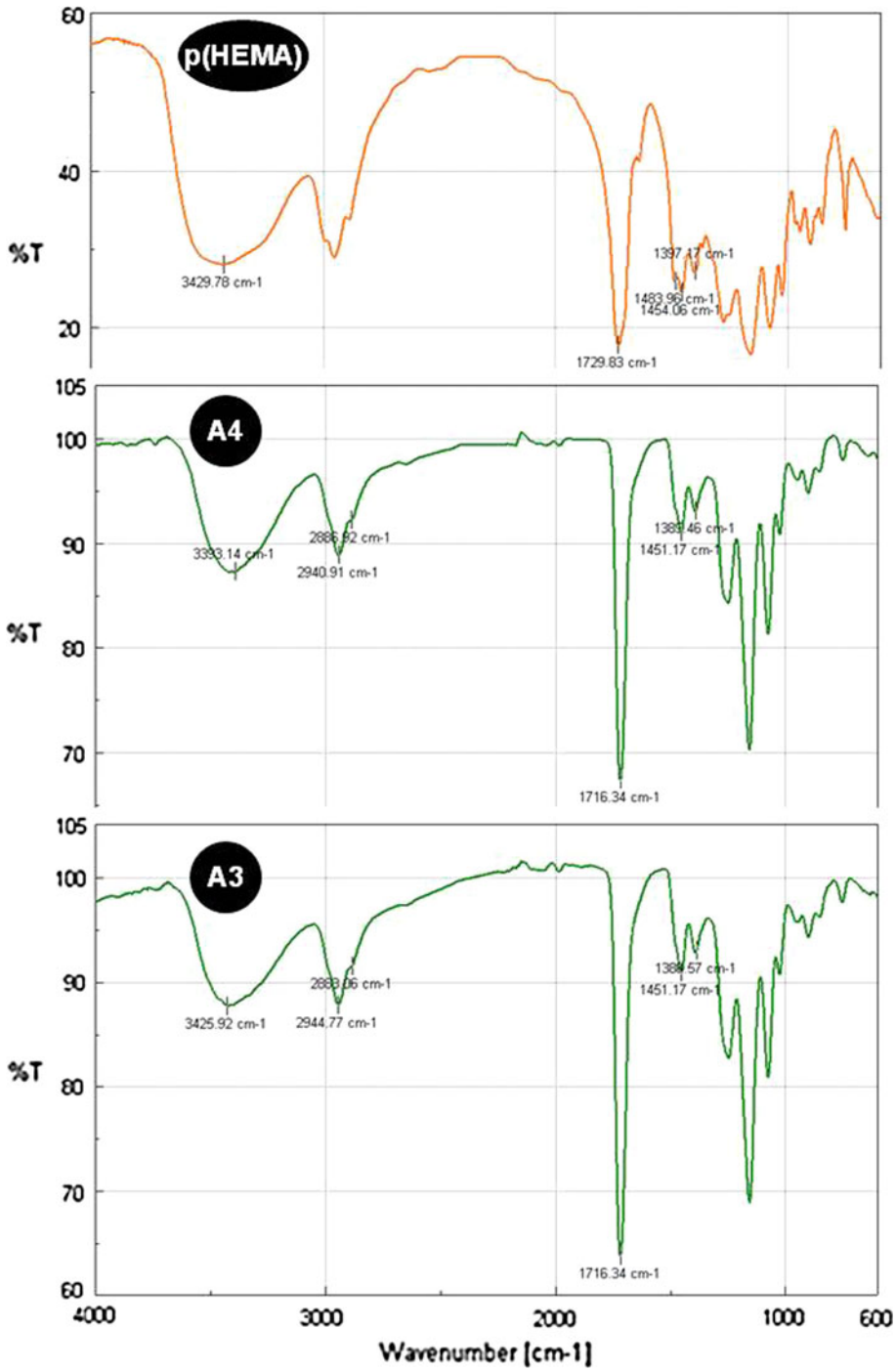

Fig. 1 FT-IR spectra of two representative terpolymers (*A3* and *A4*) compared with the spectrum of the control p(HEMA) homopolymer. The terpolymers present a stronger C=O vibration due to the presence of the carbonyl in all the three types of structural units

Further, initial rates of copolymerization can be calculated, knowing the molar composition of the copolymers obtained (Fig. 4c). The copolymerization rate increases monotonously with AA fraction in the feed. The global rate increase with AA fraction seems impossible to explain if in correlation with the values of the copolymerization ratios, which indicate a lower relative tendency for AA homopropagation. In fact, the AA acceleration effect seems to imply the "dilution" of the dDMA units responsible for mutual sterical repulsions, which increase the activation energy of dDMA homopropagation. This explanation is sustained by the relationships $r_{12} \gg r_{11}$ and $r_{12} \gg r_{22}$.

3.3.3 *Kinetic study of p(HEMA-co-dDMA-co-AA) ternary system*

In order to elucidate kinetic aspects regarding the ternary system p(HEMA-co-dDMA-co-AA), a mathematical

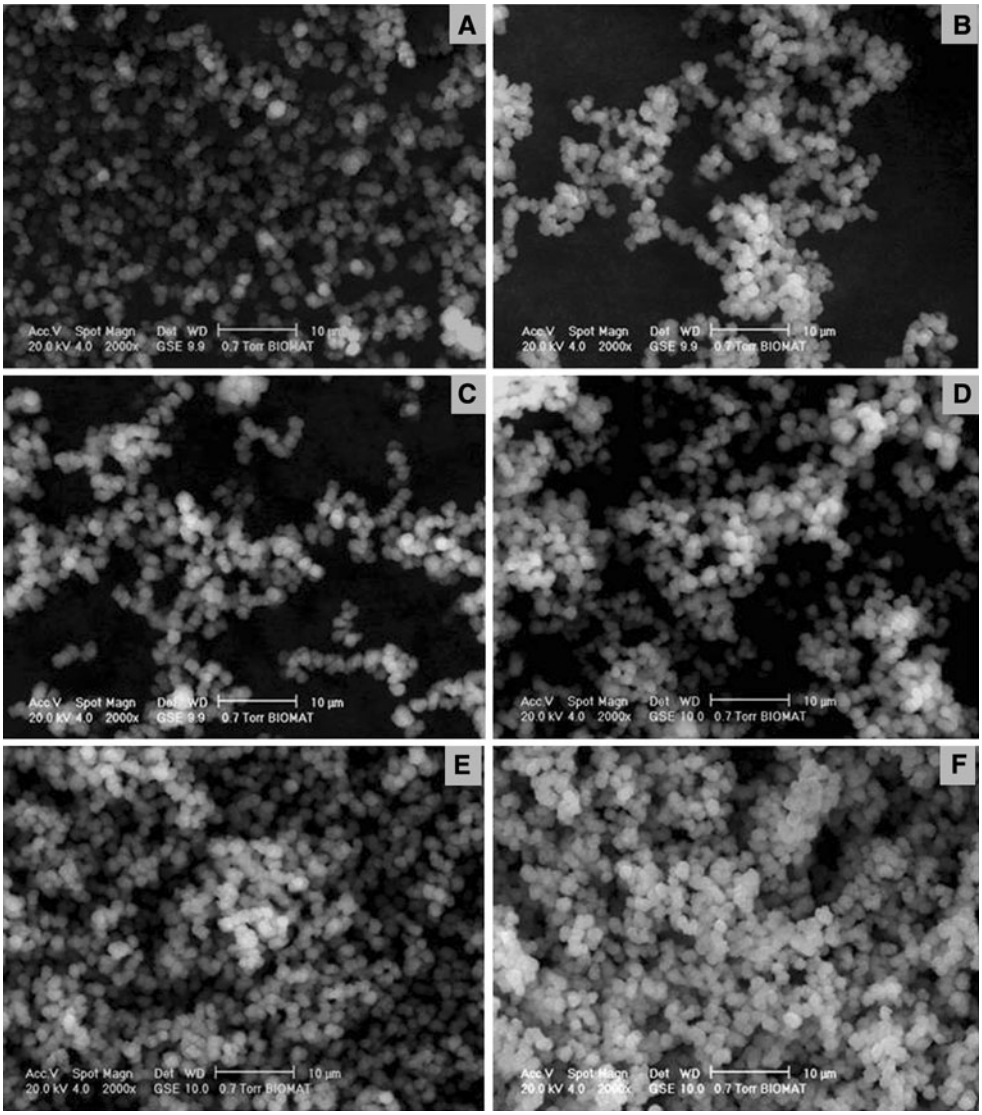

Fig. 2 SEM appearence of the obtained terpolymer particles: **a** A1, **b** A2, **c** A3, **d** A4, **e** A5, **f** A6

model of the reactivity ratios of the comonomers in the terpolymer has been created.

Notations: HEMA = M_1, dDMA = M_2, AA = M_3.

Instantaneous composition of the terpolymers depends on the six copolymerization constants and on the three instantaneous concentrations of monomers in the feed. The pairs of reactivity ratios r_{ij} and r_{ji} are also r_i and r_j from the binary copolymerization M_i/M_j.

Therefore: $r_{13} = 0.00029$; $r_{31} = 0.148$; $r_{12} = 2$; $r_{21} = 1$ [28]; $r_{23} = 0.63$; $r_{32} = 0.108$.

With these values, and, respectively with the compositions in the feed, ternary compositions diagrams have been plotted. Only HEMA-containing compositions in the feed among the limits [$x_{HEMA} = 0.75$–0.9] have been considered for the analysis, in order to maintain the terpolymer properties imposed by the medical application. Table 4 displays the values of the feed composition and instantaneous values of terpolymers composition. Further, the evolutions of the feed composition, the instantaneous and cumulative composition versus conversion, using PROCOP software, were plotted (Fig. 5). The analysis of the monomers evolutions led to the following conclusion: AA presents the highest reactivity during terpolymerisation, followed by HEMA, and dDMA, respectively.

3.4 Swelling behavior

As expected, due to the presence of dDMA, the overall water uptake of the synthesized copolymers decreases in comparison to a standard pHEMA ($\approx$55%) [29]. This behavior can be explained through the hydrophilic–hydrophobic balance in the terpolymers, namely through

Table 3 Results of the elemental analysis for the binary system HEMA-AA

Composition	Conversion (%)	t_r (min.)	Elemental analysis		
			N (%)	C (%)	H (%)
1	40.09	60	5.940	58.297	9.056
	45.05	75	0.000	49.112	9.144
	60.40	105	0.000	32.397	8.791
	64.00	135	0.009	37.825	7.615
2	46.56	60	0.000	54.330	7.687
	58.22	75	0.000	49.808	9.274
	70.17	105	0.968	49.543	8.857
	76.44	135	0.000	40.798	5.287
3	37.28	60	2.154	66.809	9.884
	55.22	75	2.453	49.498	0.000
	68.01	105	2.160	51.596	0.000
	72.25	135	2.703	44.479	0.000
4	45.26	60	0.480	48.328	7.727
	61.99	75	2.179	52.062	0.000
	63.32	105	0.076	63.719	5.450
	71.59	135	0.000	50.580	8.842

the effect of the chain constituents of different hydrophilicity. To be more specific, incorporating AA units increases the hydrophilicity potential of the polymer chain (both in the series A1, A2 and A3 obtained using 5% hydrophobic dDMA units, as in the polymer series A4, A5 and A6 obtained using 10% dDMA), while dDMA presents a strong hydrophobic behavior leading to a decrease of the water uptake in the copolymers when compared with the homopolymer. However, no significant differences in the swelling behavior were noticed for the studied compositions; the increase of the dDMA content from 5 to 10% in the polymerization mixture did not generally induce higher hydrophobicity (Fig. 6).

From a kinetic point of view, the swelling process follows a 1st order kinetic, and its evolution in terms of swelling rate is given by the equation:

$$\frac{\partial(Swelling\,Degree)}{\partial t} = k(Swelling\,Degree\,Max - Swelling\,Degree) \quad (4)$$

$$\ln\frac{Swelling\,Degree\,Max}{Swelling\,Degree\,Max - Swelling\,Degree} = kt \quad (5)$$

where the *Swelling Degree Max* is the maximum swelling degree obtained at the end of the test, t is the swelling time, k is the coefficient of the swelling rate, and *Swelling Degree* is the swelling degree at time t. Therefore, the k parameter measures the diffusion rate of the water phase in the polymer matrix (kinetic compatibility), and the maximum value of the swelling (*Swelling degree Max)* measures the thermodynamic equilibrium compatibility of the monomers in the copolymers. The constant k and the maximum swelling degree have been calculated (values not presented). Among all the terpolymers, A1 and A4 present the weakest water uptake capacity determined experimentally. Meanwhile, A1 has swollen significantly faster than all the other materials.

As a conclusion of this test, all the investigated structures present thermodynamic and kinetic compatibility with the physiological serum.

For the antibiotic-loading, three compositions with decreasing HEMA and constant dDMA content have been selected, respectively: A4 (containing 85% HEMA, 10% dDMA and 5% AA), A5 (with 80% HEMA, 10% dDMA and 10% AA), and A6 (with 75% HEMA, 10% dDMA and 15% AA).

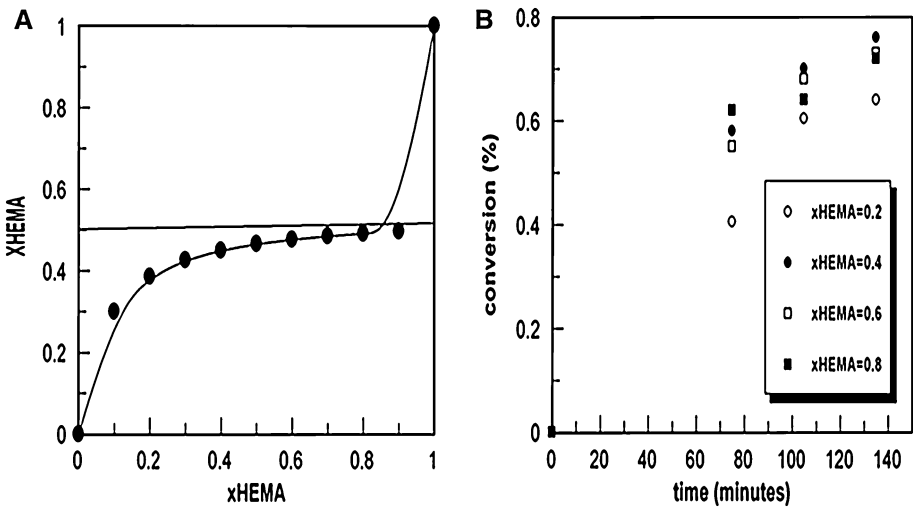

Fig. 3 The composition diagram (**a**) and the conversion vs. time (**b**) for HEMA-AA binary system

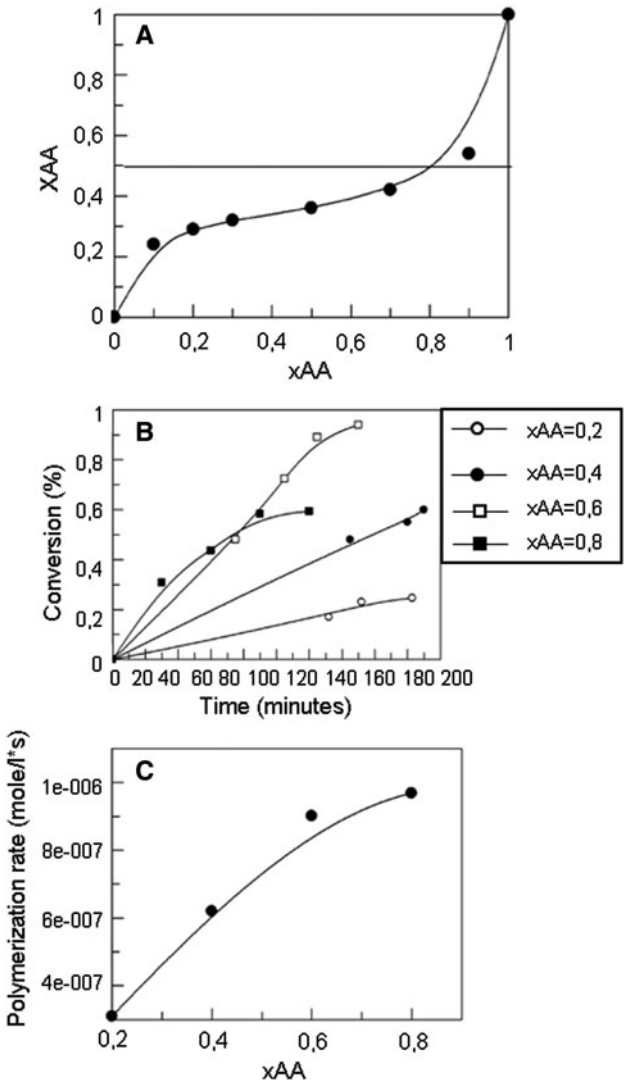

Fig. 4 The composition diagram (**a**), the conversion vs. time (**b**) and initial copolymerization rate vs. feed composition (**c**) for AA-dDMA binary system

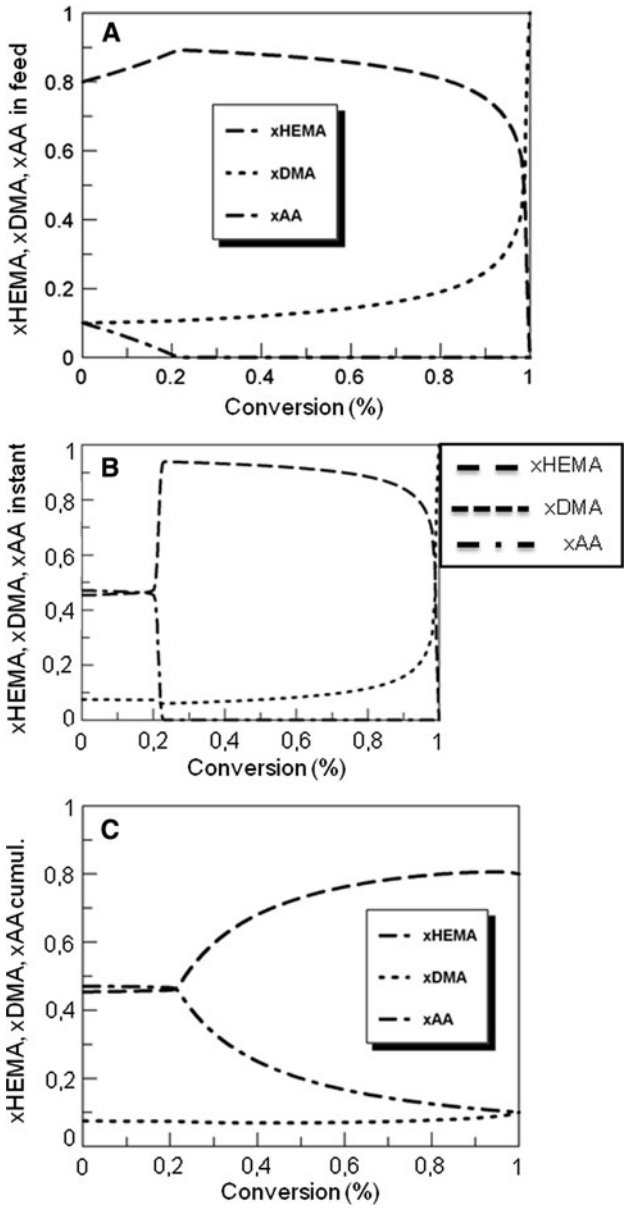

Fig. 5 Feed composition (**a**), instantaneous composition of the copolymer (**b**) and cumulative composition of the copolymer (**c**) versus conversion

Table 4 Compositions of the ternary system

xHEMA[a]	xdDMA[a]	xAA[a]	XHEMA[b]	XdDMA[b]	XAA[b]
0.9	0.05	0.05	0.48	0.0362	0.4832
0.85	0.05	0.1	0.47	0.039	0.48
0.8	0.05	0.15	0.47	0.04	0.48
0.85	0.1	0.05	0.46	0.07	0.466
0.8	0.1	0.1	0.45	0.07	0.47
0.75	0.1	0.15	0.447	0.07	0.47

[a] Feed composition

[b] Calculated terpolymer composition

3.5 NFPC coupling reaction

NFPC was chemically attached to the terpolymers synthesized by a transesterification reaction. The water produced was absorbed by DCC, and *N*,*N*′-dicyclohexylurea resulted was removed. The FT-IR analysis has given the qualitative expression of the success of the drug immobilization. As expected, the drug-treated polymers presented spectral details characteristic both to the carrier as well to the NFPC. All the spectra of the polymers submitted to the antibiotic modification have presented a new specific peak at 1569 cm^{-1}, assigned as the N–H II band from NFPC. Nevertheless, the peak at around 3400 cm^{-1} is broader in all the drug-treated polymers when compared to the unmodified terpolymers, suggesting a coupled influence of the O–H stretching vibration from the polymer

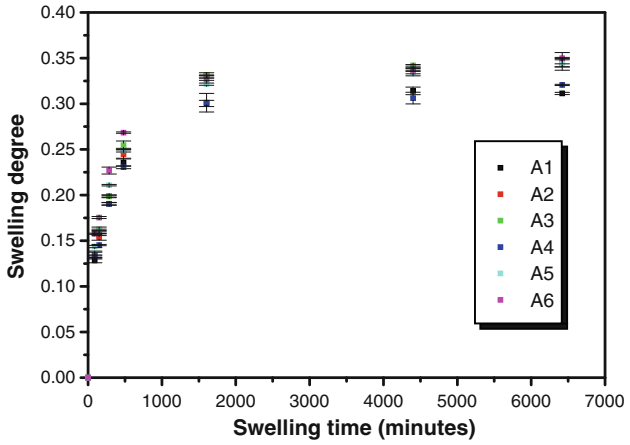

Fig. 6 The swelling degree for the obtained terpolymers, *A1–A6*, in saline, over time; the maximum swelling degree is 35%; STDV < 0.005

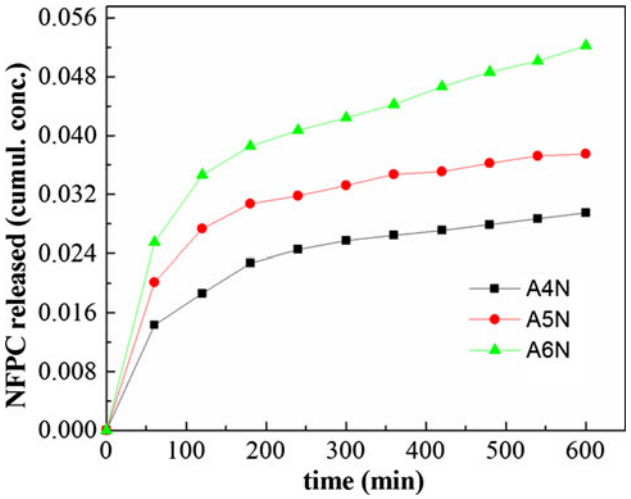

Fig. 7 Quantitative expression of the in vitro NFPC release from *A4 N*, *A5 N*, *A6 N* microbeads, presented as the cumulative concentration of NFPC in the testing saline solution, over time. The drug is released during the first 6 h

substrates and of the N–H from the secondary amide in NFPC (spectra not shown).

The quantitative assessment of the NFPC content in the terpolymers has been performed through UV–Vis spectroscopy, by the monitoring of the NFPC released from a known amount of modified polymer. NFPC-terpolymer weight ratios in the feed were 1:2. The incorporation efficiency was expressed as the ratio of the amount of NFPC incorporated in the microbeads over the total amount of NFPC used in the coupling reaction. Drug content was calculated as the ratio of the drug in the microbeads over the total initial amount of the polymer. Approximately the whole amount of NFPC was loaded into A6 N (98%), while the loading efficiencies of the other two samples were 77.5% in case of A4 N, and 92.5% for A5 N, respectively.

Additionally, SEM investigation has proven that the NFPC-treated beads do not show any relevant modification in size or shape, keeping the original spherical shape and dimension (images not shown).

3.6 In vitro NFPC release

The quantitative expression of the antibiotic release from the studied polymer substrates has been achieved through UV–Vis spectroscopy. Briefly, the evolution in time of the drug specific absorbance at 330 nm has been monitored. The amount of drug released at any time (M_t) has been calculated from the calibration curve obtained with saline aqueous solutions of NFPC from 0.001 mg/ml to 0.1 mg/ml. The calibration coefficient obtained was 0.99986, with the maximum error ±0.0014, and the linear expression of the calibration:

$$\text{Conc.} = +0.188278 \times \text{Absorbance} - 1.34576\text{e} - 011$$

The kinetics of NFPC release from A4 N, A5 N and A6 N microbeads are presented in Fig. 7, where M_t is the molar amount of drug released at time t and M_∞ is the maximum molar amount of drug released at equilibrium, which reached the important values of drug loading.

As Arifin described [30], in order to simplify the analysis of controlled release data from polymeric devices of varying geometry, an empirical, exponential expression has been developed to relate the fractional release of drug to the release time:

$$\frac{M_t}{M_\infty} = kt^n \tag{6}$$

where M_t/M_∞ is the fractional solute release, t is the release time, k is a constant, and n is the exponent characteristic of the release mechanism.

This equation applies until 60% of the total amount of drug is released. It predicts that the fractional release of drug is exponentially related to the release time and it adequately describes the release of drug from slabs, spheres, cylinders and discs from both swellable and non-swellable matrices. The slope (n) of the log (drug released) versus log (time) plot is 0.5 for pure Fickian diffusion.

An anomalous non-Fickian diffusion pattern ($n = 0.5$–1 or $n = 0.45$–0.89) is observed when the rates of the solvent penetration and drug release are in the same range. This deviation is due to increasing drug diffusivity in the matrix by the solvent induced relaxation of the polymers. Zero order drug release ($n = 0.89$ or $n = 1$) is achieved when drug diffusion is rapidly compared to the constant rate of solvent induced relaxation and swelling in the polymer (Case II transport for swellable polymers). Use of this equation to analyze data of drug release from a porous system will probably lead to $n < 0.5$, since the combined mechanisms (diffusion through the matrix and partially

through water-filled pores) will shift the release exponent toward smaller values [1, 31, 32]. In consequence, graphs of ln (M_t/M_∞) versus ln t were plotted in order to obtain the slope (value of n). The study conducted to values of n close to 0.3 (Fig. 8), which means that, in this case, the mechanism followed is case "$n < 0.5$", where the release takes place from a porous material.

The results presented in Figs. 7 and 8, describing the amount of NFPC released from the p(HEMA-co-dDMA-co-AA) microbeads as a function of time, show good agreement with what we expected: the amount released depends upon the initial amount of the drug present in the polymer matrix, which, on its turn, depends not only on the HEMA ratio, but also on the AA ratio in the polymer backbone.

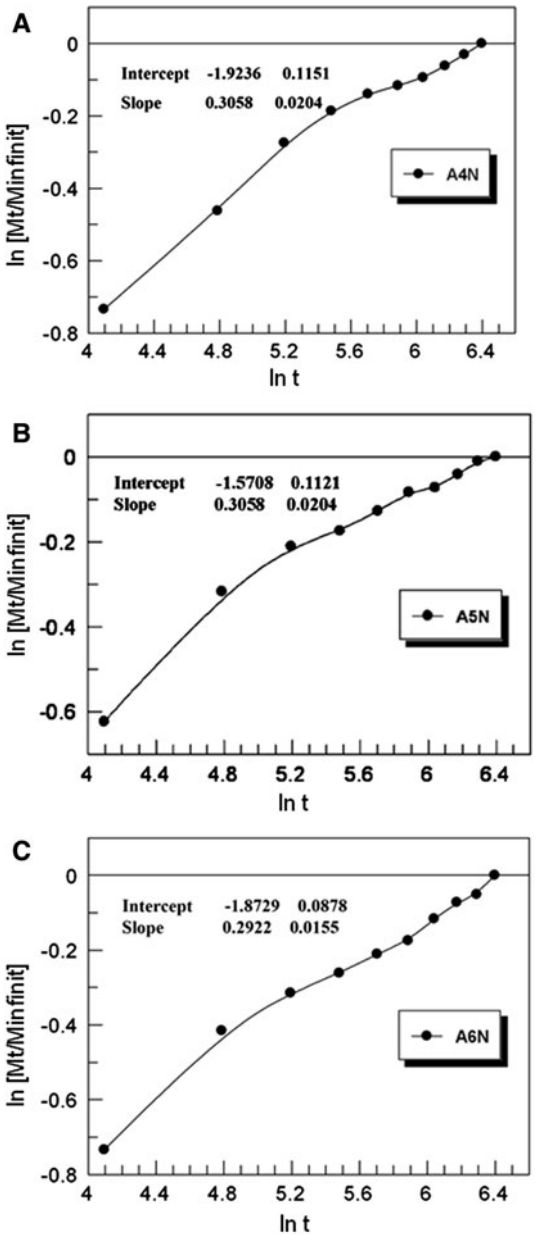

Fig. 8 Diagrams presenting the kinetic mechanism of the NFPC release from: **a** A4 N; **b** A5 N; **c** A6 N

3.7 In vitro cellular tests

All the compositions obtained were submitted to cytotoxicity and viability tests. The cells were examined by inversion microscopy, before and after the incubation with the samples. No cytotoxic effects have been observed, the morphologic characteristics and the adherence being similar for the cells incubated in the presence or in the absence of the samples. In the same time, after the addition of the MTT dye, both the cells incubated with the samples and those untreated have reduced the MTT and have formed formazan crystals.

After the dissolution of the formazan crystals, the optical density was measured at 570 nm. The cellular viability has been calculated in percentage versus a blank control test (with cells incubated in the same conditions and volume). Cellular viability, given as average ± standard deviation of viability ratios obtained from three experiments for each molar ratio of terpolymer versus the control sample, has been found to be: 97.7 ± 1.29% for A1; 97.4 ± 1.34% for A2; 97.9 ± 1.19% for A3; 98.2 ± 0.78% for A4; 98.1 ± 0.92% for A5, and 97.8 ± 1.22% for A6, in case of maximum stimulation volume.

The in vitro tests of cytotoxicity made on fibroblast murine L929 cell line gave adequately results for all the compositions tested, p(HEMA-co-dDMA-co-AA) compositions being considered to present minimal adverse effects on cell morphology and viability.

4 Conclusion

In the present paper, the synthesis of p(HEMA-co-dDMA-co-AA) terpolymers as 1 μm-microbeads was presented. The kinetic expression of HEMA-AA and dDMA-AA binary systems was determined. Reactivity ratios were obtained for: the system HEMA-AA: $r_1 = 0.00029$, $r_2 = 0.148$; the system AA-dDMA: $\overline{r_1} = 0.108$; $\overline{r_2} = 0.63$. On the basis of these values, instantaneous and cumulative p(HEMA-co-dDMA-co-AA) terpolymer compositions versus conversion were estimated.

This information is extremely useful in the view of determining the AA content in any moment of the reaction, for any initial composition in the feed, responsible for the NFPC covalently bond to the polymer and further released in the organism. The efficiency of the drug loading and the in vitro release kinetics were determined on three

compositions NFPC-loaded. Two of the compositions, 80:10:10 and 75:10:15 M compositions, present valuable opportunities for further in vivo testing, in order to be used as drug delivery systems in treatment of different osseous diseases.

Acknowledgments Professor Georgios Staikos from University of Patras is gratefully acknowledged for his kind support with the elemental analysis. The project PN II IDEAS 729/2009 *Polymer biomaterials for bone regeneration. Biomimetism through surface nanostructing* is gratefully acknowledged.

References

1. Brannon-Peppas L. Recent advances on the use of biodegradable microparticles and nanoparticles in controlled drug delivery. Int J Pharm. 1995;116:1–9.
2. De Wit M, Raabe A, Tuinmann G, Hossfeld DK. Implantable device for intravenous drug delivery in the rat. Lab Anim. 2001;35:321–4.
3. Branco MC, Schneider JP. Self-assembling materials for therapeutic delivery. Acta Biomater. 2009;5:817–31.
4. Kim S, Kim J-H, Jeon O, Kwon IC, Park K. Engineered polymers for advanced drug delivery. Eur J Pharm Biopharm. 2009;71:420–30.
5. Elvira C, Gallardo A, San Roman J, Cifuentes A. Covalent polymer-drug conjugates. Molecules. 2005;10:114–25.
6. Rezwan K, Chen QZ, Blaker JJ, Boccaccini AR. Biodegradable and bioactive porous polymer/inorganic composite scaffolds for bone tissue engineering. Biomaterials. 2006;27:3413–31.
7. Nair LS, Laurencin CT. Polymers as biomaterials for tissue engineering and controlled drug delivery. Adv Biochem Eng/Biotechnol. 2006;102:47–90.
8. Ringsdorf H. Structure and properties of pharmacologically active polymers. J Polym Sci Polym Symp. 1975;51:135–53.
9. Norden CW, Bryant R, Palmer D, Montgomerie JZ, Wheat J. Chronic osteomyelitis caused by *Staphylococcus aureus*: controlled clinical trial of nafcillin therapy and nafcillin-rifampin therapy. South Med J. 1986;79:947–51.
10. Pillai RR, Somayaji SN, Rabinovich M, Hudson MC, Gonsalves KE. Nafcillin-loaded PLGA nanoparticles for treatment of osteomyelitis. Biomed Mater. 2008;3:034114.
11. Lacey RW, Stokes A. Susceptibility of the "penicillinase-resistant" penicillins and cephalosporins to penicillinase of *Staphylococcus aureus*. J Clin Pathol. 1977;30:35–9.
12. Sato K, Lin TY, Weintrub L. Bacteriological efficacy of nafcillin and vancomycin alone or combined with rifampicin or amikacin in experimental meningitis due to methicillin-susceptible or -resistant *Staphylococcus aureus*. Jpn J Antibiotics. 1985;38:2155–62.
13. Katime I, Sáez V, Hernáez E. Nafcillin release from poly(acrylic acid–co–methyl methacrylate) hydrogels. Polym Bull. 2005;55:403–9.
14. Chan V. Influence of temperature and drug concentration on nafcillin precipitation [1]. Am J Health-System Pharm. 2005;62:1347–8.
15. Katime I, Valderruten N, Quintana JR. Controlled release of aminophylline from poly(*N*-isopropylacrylamide-co-itaconic acid) hydrogels. Polym Int. 2001;50:869–79.
16. Duncan R. Drug-polymer conjugates: potential for improved chemotherapy. Anti-Cancer Drugs. 1992;3:175–210.
17. Duncan R. Polymer conjugates for tumour targeting and intracytoplasmic delivery. The EPR effect as a common gateway? Pharm Sci Technol Today. 1999;2:441–9.
18. Putman D, Kopecek J. Polymer conjugates with anticancer activity. Adv Polym Sci. 1995;122:55–123.
19. Mabilleau G, Stancu IC, Honore T, Legeay G, Cincu C, Basle MF, Chappard D. Effects of the length of crosslink chain on poly(2-hydroxyethyl methacrylate) (pHEMA) swelling and biomechanical properties. J Biomed Mater Res A. 2006;77:35–42.
20. Sharma S, Nijdam AJ, Sinha PM, Walczak RJ, Liu X, Cheng MM-C, Ferrari M. Controlled-release microchips. Expert Opin Drug Deliv. 2006;3:379–94.
21. Wu P, Grainger DW. Drug/device combinations for local drug therapies and infection prophylaxis. Biomaterials. 2006;27:2450–67.
22. Merz E, Alfrey T, Goldfinger G. Intramolecular reactions in vinyl polymers as a means of investigation of the propagation step. J Polym Sci A. 1996;34:5–12.
23. Babazadeh M. Synthesis, characterization, and in vitro drug-release properties of 2-hydroxyethyl methacrylate copolymers. J Appl Polym Sci. 2007;104:2403–9.
24. Zecheru T, Filmon R, Rusen E, Marculescu B, Zerroukhi A, Cincu C, Chappard D. Biomimetic potential of some methacrylate-based copolymers: a comparative study. Biopolymers. 2009;91:966–73.
25. Mayo FR, Lewis FM. Copolymerization I. A basis for comparing the behavior of monomers in copolymerization; the copolymerization of styrene and methyl methacrylate. J Am Chem Soc. 1944;66:1594–601.
26. Hagiopol C. Copolymerization: toward a systematic approach. New York: Kluwer-Academic/Plenum; 1999.
27. Berger M, Kuntz I. The distinction between terminal and penultimate copolymerization models. J Polym Sci A. 1964;2:1687–98.
28. Ito K, Uchida K, Kitano T, Yamada E, Matsumoto T. Solvent effects in radical copolymerization between hydrophilic and hydrophobic monomers; 2-hydroxyethyl methacrylate and lauryl methacrylate. Polym J. 1985;17:761–6.
29. Denizli A, Garipcan B, Karabakan A, Senöz H. Synthesis and characterization of poly(hydroxyethyl methacrylate-*N*-methacryloyl-(L)-glutamic acid) copolymer beads for removal of lead ions. Mater Sci Eng C. 2005;25:448–54.
30. Arifin DY, Lee LY, Wang C-H. Mathematical modeling and simulation of drug release from microspheres: implications to drug delivery systems. Adv Drug Deliv Rev. 2006;58:1274–325.
31. Serra L, Doménech J, Peppas NA. Drug transport mechanisms and release kinetics from molecularly designed poly(acrylic acid-g-ethylene glycol) hydrogels. Biomaterials. 2006;27:5440–51.
32. Mackerle J. Finite-element analysis and simulation of polymers: a bibliography (1976–1996). Model Simul Mater Sci Eng. 1997;5:615–50.